Dynamic Quantitative Susceptibility Mapping for Contrast Agent Concentration

Bo Xu[1], Tian Liu[2], Pascal Spincemaille[2], Nandadeepa Thimmappa[2], Martin R Prince[2], and Yi Wang[1]
[1]*Biomedical Engineering, Cornell University, Ithaca, New York, United States,* [2]*Weill Cornell Medical College, New York, New York, United States*

TARGET AUDIENCE: anyone interested in quantification of contrast agent biodistribution and susceptibility

PURPOSE: Quantitative susceptibility mapping (QSM) promises to quantify contrast agent biodistribution, which is of great interest to understand tissue pathophysiology. Current QSM requires 3D multi-echo gradient echo (GRE) acquisition that takes at least several minutes, but contrast agent dynamic biodistribution changes on a sub-second time scale. High temporal-spatial resolution 4D imaging can be obtained using temporal resolution acceleration with constrained evolution reconstruction (TRACER)[1]. To achieve high temporal-spatial resolution QSM, we have developed a multi-echo spiral GRE sequence with TRACER reconstructed complex images to quantify gadolinium agent passage in vasculature. Complex images are processed with a morphology enabled dipole inversion with nonlinear formulation (MEDIN)[2] to generate dynamic 3D gadolinium concentration ([Gd]) map.

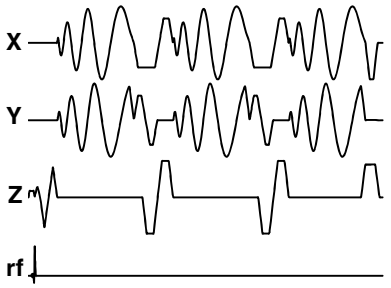

Fig. 1 Multi-echo spiral GRE sequence

METHODS: ***Pulse sequence:*** A 3-echo 3D stack spirals GRE sequence was developed (Fig.1) with gradient moment nulling on all axes. Consecutive spiral leaves were rotated over the golden ratio angle. ***Data acquisition:*** N=7 healthy volunteers were scanned using an 8-channel head coil. Fifteen ml of Magnivist (0.5M) injection at 1ml/s was initiated 20s after scan start. TR/TE_{min}/TE_{max} = 23.4/3.2/18.3 ms, FA=10°, BW=±125KHz, matrix size = 240×240×28, voxel size = 1×1×2.5mm^3. ***3-echo complex image frame:*** the MR signal equation at frame n could be written as $y_n = E_n(x_n)$ where y_n is the acquired k-space data, E_n is the encoding function and x_n is the complex frame image. Then $x_n = argmin_{x_n} \|y_n - E_n(x_n)\|^2 + \mu\|x_n - x_{n-1}\|^2$, using the previous frame to constrain the current frame under the approximation of small change between consecutive frames[1,2], achieving sub-second temporal 3D frame rate. ***Dynamic QSM:*** Background was removed via temporal subtraction from a reference frame prior to Gd arrival. Then the 3-echo 3D complex frame was input for a subsequent quantitative susceptibility mapping solver MEDIN[2]. [Gd] was obtained by scaling the susceptibility map with the Gd^{3+} mol susceptibility (308 ppm/mol).

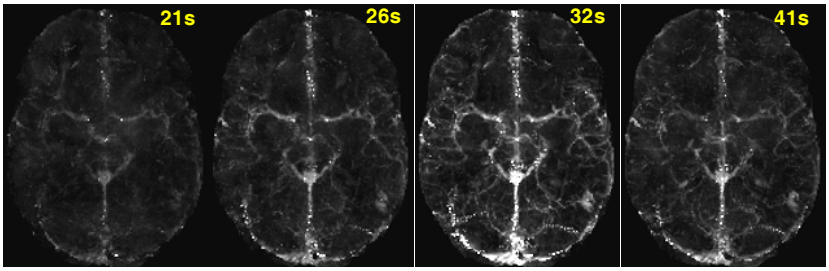

Fig. 2 Axial MIPs of Gd concentration at four time points

RESULTS: In all volunteers, 0.6 second frame rate QSM images were successfully obtained. Fig. 2 shows axial MIPs of 4 QSM frames after Gd injection. Enhancement of both arteries and veins at different stages was well observed. Fig.3 shows two representative slices of QSM image at 30s. The Gd concentration time course of the middle cerebral artery (MCA) and straight sinus (SS) are plotted in Fig 4. The bolus concentration immediately after Gd injection is roughly about 5mmol/L under 1ml/s injection rate and 6L/min cardiac output, which is in agreement with our measured peak [Gd] value in artery (3mmol/L), with the discrepancy likely due to the dispersion of the bolus and partial volume effects.

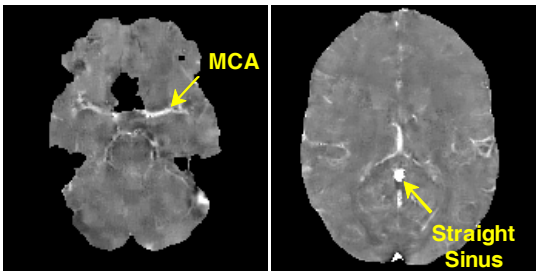

Fig. 3 QSM image at 30s, shown are vessels used to plot Gd concentration curve

DISCUSSION AND CONCLUSION: We present a dynamic QSM technique for 3D [Gd] mapping at sub-second frame rate. The mapped arterial [Gd] agrees with injection rate. This technique may be used in perfusion MRI, which currently suffers from the lack of absolute [Gd] quantification due to the nonlinear relationship between signal intensity and [Gd]. Dynamic QSM can provide quantitative arterial input function and venous input function for quantitative perfusion imaging that is important for studying various diseases including acute stroke and tumor.

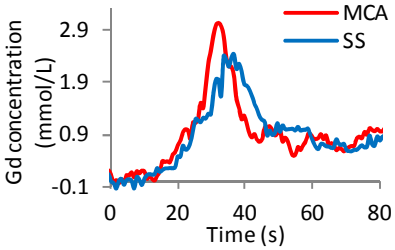

Fig. 4 AIF and VOF curve

REFERENCES: [1] Xu et al. MRM, 2012, DOI: 10.1002/mrm.24253. [2] Liu et al. MRM, 2012, DOI: 10.1002/mrm.24272. [3] Uecker et al. MRM, 2008, 60:674-682.